Bulletin of Earthquake Engineering (2019) 17:1379–1406
https://doi.org/10.1007/s10518-018-0500-z

ORIGINAL RESEARCH

Rapid seismic assessment of two four-storey R.C. test buildings

Stylianos I. Pardalopoulos[1,2] · **Stavroula J. Pantazopoulou**[3]

Received: 31 July 2018 / Accepted: 11 October 2018 / Published online: 16 October 2018

Abstract
Seismic evaluation of existing reinforced concrete buildings that are classified as non-conforming to modern earthquake standards is an urgent priority, since this class of buildings represents the majority of the built environment throughout the world. To address this need a simple procedure for rapid seismic assessment (RSA) of the earthquake demand and available capacity of existing buildings has been devised and calibrated through field applications. RSA is based on first principles, considering the prevalent failure modes of the load bearing components of the structure, and easily accessible information regarding the geometric and material characteristics of the structure. In this paper the RSA method is further improved by introducing expressions for direct estimation of the local drift demands of the examined building at peak seismic response using the structure's unique geometric and material properties. The accuracy of the RSA procedure is evaluated through application and comparison of the assessment results with the recorded seismic responses of two model experimental structures that had been tested under pseudo dynamic loads simulating earthquake effects, reported in the literature. The example structures were chosen because they were full-scale structures with relatively simple layout (planar frames), in order to develop an instructive paradigm of the RSA's application for the interest of practitioners.

Keywords Seismic assessment · Performance · Earthquake engineering · Existing construction

✉ Stylianos I. Pardalopoulos
stylpard@gmail.com

Stavroula J. Pantazopoulou
pantazo@yorku.ca

[1] School of Civil Engineering, Aristotle University of Thessaloniki, Thessaloniki, Greece

[2] Institute of Engineering Seismology and Earthquake Engineering, Thessaloniki, Greece

[3] Department of Civil Engineering, Lassonde Faculty of Engineering, York University, Toronto, ON, Canada

1 Introduction

The vast inventory of the build environment worldwide is classified as *existing* construction. Every building sample is unique in that it represents a different state of service condition and maintenance, but it may also be characterized by the resilience inherited from the design code framework at the time of construction. Yet, from among this multitude of individual cases, older structures built prior to the 1980s, when a major shift occurred in earthquake engineering design philosophy, share common types of deficiencies, the primary ones being a lack of ductility combined with unfavourable distribution of stiffness. Strong earthquakes in the past that struck urban areas (Loma Prieta 1989, Northridge 1994, Kobe 1995, Kocaeli 1999, Athens 1999, Bhuj 2001, Port-au-Prince 2010, Gorkha 2015, Mexico City 2017) highlighted the vulnerability of many of the existing reinforced concrete (R.C.) buildings, particularly structures built several decades ago according to obsolete design standards (if at all) which would be considered deficient and substandard according to the current state of design practice (Fig. 1). Seismic deficiency may also result from bad maintenance and the deleterious effects of aggressive environmental exposure: thus, it is a pressing societal priority to develop diagnostic procedures that may quickly identify such structures that are likely to collapse in a future earthquake event. A corollary is the need to quantify the level of earthquake intensity (peak ground acceleration—PGA) that existing construction with deficiencies in its structural system may tolerate prior to collapse.

Extensive research has been conducted over the past three decades aiming to predict the damages that may occur to existing R.C. buildings during strong earthquakes. These studies have resulted in the development of many different assessment procedures. Regardless of their identifying characteristics, these procedures may be classified into three major categories depending on the knowledge level regarding material, building geometry and structural properties that are required as input for conducting the assessment, thereby defining the accuracy of the produced results. These are known as first-, second- and third-level assessment procedures.

The first-level assessment procedures (FEMA P-154 2015; IEP Assessment 2017, etc.) are developed for rapid visual screening of large numbers of buildings. They focus on evaluation of the vulnerability of the existing building stock based on statistical analyses of the seismic response of typologically and structurally similar buildings during past strong earthquakes. These procedures, which usually are meant to be used by field inspectors of a wide range of occupations (civil engineers, structural engineers, architects, design professionals, building officials, construction contractors, firefighters, etc.), involve a sidewalk survey and the filling of a data collection form, according to which the examined buildings

Fig. 1 Brittle failures of R.C. buildings in Greece due to earthquake actions

are ranked with a global vulnerability score that classifies them as safe, or, potentially dangerous, requiring a more detailed seismic assessment.

The second-level assessment procedures (JBDPA Standard 2001; Gülkan and Sozen 1999; Gür et al. 2009; Thermou and Pantazopoulou 2011; Yakut et al. 2005; Yakut 2004) include more complex investigation of the seismic response of the examined building. Similarly to the first-level assessment, procedures of this category are developed for in situ screening of potentially hazardous buildings, although they generally require more computational time. The second-level assessment procedures allow for the estimation of potential damages during an earthquake scenario for individual structural members of the examined building, as well as for the entire building, based on simple calculations requiring the knowledge of geometrical and material properties. Furthermore, assessment procedures of this category are mainly addressed to specialized structural engineers, knowledgeable in identifying the structural characteristics of the examined buildings. To this end, second-level assessment procedures provide a more detailed insight on the seismic response of the examined structure by approximating its seismic capacity in terms of damage indices, without losing the capability of rapid application to existing buildings.

The third-level assessment procedures (EN 1998-3 2005; Greek Code of Structural Interventions 2012; FEMA-356 2000; Vamvatsikos and Cornell 2002; Kappos et al. 2006) require detailed seismic analysis of the examined buildings using elastic and/or inelastic analysis procedures. Although advanced numerical tools may be used towards such an objective, they generally require a high level of specialization and access to expensive software, field diagnostic tools and a commensurate budget. Therefore, third-level assessment of existing buildings yields results of the upmost possible detail in terms of seismic response and capacity, yet, due to budgetary constraints, they can only be performed for a limited number of buildings.

Acknowledging the need for an assessment strategy that can be easily applicable for assessment of large numbers of existing R.C. buildings, which would also allow for quantification of the seismic resistance of the examined structure, Pardalopoulos et al. (2013, 2018a) developed a simple methodology. Because it gives quantitative results, the method may be used both for evaluation of reinforced concrete structures but can also lead to the selection of the appropriate retrofit strategy if inadequate seismic resistance is diagnosed. The procedure subsequently evolved into a system of seismic rating of existing buildings known as RSA (for *Rapid Seismic Assessment procedure for R.C. buildings*). Through the method, the base shear coefficient available to the building is estimated, along with the expected ductility demand and the likely damage scenario to be experienced in the design seismic hazard. The assessment procedure has been calibrated through application to many collapsed as well as non-collapsed older substandard buildings that have gone through significant seismic events. Using the method the likely mode of failure of the building may be identified, the expected damage, and the pattern of damage localization to the most critical members. The method is powerful in that it may help to identify those aspects of structural detail, or geometry, which are primarily responsible for increasing the seismic vulnerability of the structure, and may also be used to guide retrofitting of deficient structures through reverse-engineering of their response.

In this paper, an improved version of the RSA procedure is presented. The improvements refer to the introduction of expressions for direct calculation of the local drift demands of the examined building at the estimated peak seismic response using the structure's unique geometric and material properties. Furthermore, in the second section of the paper, an example illustration of the RSA procedure that could serve as a guide for interested users is presented in the cases of two full-scale, experimental structures, representative of the

design and construction practice used until the early 1980's, which were constructed and tested under a sequence of ground motions in the ELSA laboratory (Varum 2003).

2 Rapid seismic assessment of R.C. buildings

The Rapid Seismic Assessment procedure (RSA) was intended as a practical diagnostic tool for rapid screening of R.C. buildings. For this reason, the procedure uses information that is most readily available upon site inspection, such as the geometric properties of the building (number of floors, typical clear floor height, area per floor including the balconies, location in plan and gross geometry of load carrying members, location, orientation and dimensions of masonry infills), as well as the reinforcement details and the material properties of the structural elements, based on the typical properties that were used in the era of construction, or, from non-destructive tests. This information is then processed through a two-criteria process, referred to as the *Stiffness Assessment Criterion*, and the *Strength Assessment Criterion* which, utilizing simple principles of structural mechanics, combined provide of a quick estimate of the buildings' seismic response. The *Stiffness Assessment Criterion* determines the total lateral drift demand of the building, and the local demands in the individual floors and components (Shiga et al. 1968; Gülkan and Sozen 1999; Thermou and Pantazopoulou 2011); it can be used to gauge possible lack of stiffness, or stiffness irregularities. With the *Strength Criterion* it is determined whether the local drift demands can be tolerated without failure along the load resistance path. Criteria to assess the stiffness and thereby the demand have been derived in many different forms and using different assumptions and simplifications by many design/assessment standards such as the Japanese assessment method (JBDPA 2001). Greater discord exists among different ways of defining the various competing strength mechanisms. A distinguishing, identifying aspect of the strength criterion of the present work is the use of a pertinent static system that enables ordering of the various mechanisms of resistance so as to identify the weakest link that controls behavior. Clearly a more detailed assessment is called for in those cases which, upon preliminary evaluation, are found deficient and unsafe for the current intensity of seismic hazard in the region of interest.

2.1 Stiffness assessment criterion

To determine the seismic demand that a future seismic event may impose on a building it is required to (a) define the seismic hazard for the region of interest, and (b) estimate the representative fundamental period of the structure that dominates the response. For lack of other easily accessible information of seismicity the design spectrum of the region of interest is used to quantify the hazard (e.g. a smooth Code acceleration spectrum with a PGA value that is associated with 2% probability of exceedence in 50 years).

It is well established from basic principles of structural dynamics that the fundamental period of lateral translation, the equivalent lateral stiffness and mass of the equivalent generalized Single Degree of Freedom (ESDOF) representing the structure are all related through the predominant (fundamental) shape of lateral response, $\tilde{\boldsymbol{\Phi}}$ (Clough and Penzien 1975). This shape is approximated here by the normalized deflection profile of the examined building at the instant of its peak seismic response in the direction of the earthquake excitation. Total lateral drift ratio of the entire building, θ_{tot}, is defined by the displacement demand at the top of the building, divided by the building height. Localization of drift demand refers to the points

in the structure where the relative drift ratio exceeds the value of θ_{tot}. However, it is important to note that this tendency for localization is already embedded in the spatial distribution of $\tilde{\boldsymbol{\Phi}}$.

In the case of multistorey R.C. buildings an approximation of the fundamental translational mode of vibration for structures up to four storeys high may be defined with reference to the translational storey mass and stiffness, M_i and K_i ($i=1\div4$), from the expression of Eq. (1) [this is derived from Rayleigh's method (Clough and Penzien 1975)], or, in detailed form in Table 1 (assuming constant storey mass), whereas, if a lower soft storey exists (pilotis-type buildings) then a simplified assumption of the fundamental translational mode of vibration is $\Phi_i=1$.

$$\tilde{\Phi}_i=\frac{\Phi_i}{\Phi_{\max}};\ \Phi_i=\frac{1}{N}\cdot\sum_{j=1}^{i}\frac{1}{K_j}\cdot\sum_{\ell=j}^{N}\ell\cdot M_\ell;\ \Phi_{\max}=\frac{1}{N}\cdot\sum_{j=1}^{N}\cdot\frac{1}{K_j}\cdot\sum_{\ell=j}^{N}\ell\cdot M_\ell;\ \Delta\Phi_j=\frac{1}{N\cdot K_j}\cdot\sum_{\ell=j}^{N}\ell\cdot M_\ell \tag{1}$$

where, N is the number of storeys in the building.

For buildings with a uniform plan configuration with typical arrangement of R.C. columns in plan (e.g.: one column per 10 m^2 of storey plan) and masonry infills without openings (windows or doors), the storey lateral stiffness, K_i, may be calculated from Eq. (2a) (Pardalopoulos et al. 2018b):

$$K_i=\left(A_f/H_{cl}\right)\cdot D_i^c\cdot\rho_i,\quad\text{where }\rho_i=\rho_{c,i}+\frac{D_i^{\inf}}{D_i^c}\cdot\rho_{\inf,i} \tag{2a}$$

whereas for buildings with N_c columns with a non-typical plan arrangement and N_{inf} infill masonry piers (Fig. 2), if rigid diaphragms may be assumed, it may be shown that (Pardalopoulos et al. 2018b):

$$K_i=\sum_{j=1}^{Nc}\alpha_{c,j}\cdot\frac{E_c}{H_{cl}}\cdot A_{col,j}\cdot\left[\frac{h_j}{H_{cl}}\right]^2+\sum_{k=1}^{N\inf}\frac{A_{\inf,k}}{H_{cl}}\cdot\frac{0.10\cdot f_{\inf,k}}{\mu_{y,k}^{\inf}\cdot\theta_{y,k}^{\inf}\cdot\sqrt{1+H_{\inf,k}^2/L_{\inf,k}^2}} \tag{2b}$$

Table 1 Expressions used for estimating the deflected shape of 2-, 3- and 4-storey R.C. buildings with constant storey mass at the instant of their peak seismic response [derived from first principles, after application of Rayleigh's method (Clough and Penzien 1975)]

# of storeys	Deformed shape	Auxiliary terms
2	$\tilde{\boldsymbol{\Phi}}=\left\{\begin{array}{c}1\\ \frac{1}{Q_2}\cdot\left(1.5\cdot K_2\right)\end{array}\right\}$	$Q_2=1.5\cdot K_2+K_1$
3	$\tilde{\boldsymbol{\Phi}}=\left\{\begin{array}{c}1\\ \frac{1}{Q_3}\cdot\left(2\cdot K_2\cdot K_3+1.67\cdot K_1\cdot K_3\right)\\ \frac{1}{Q_3}\cdot\left(2\cdot K_2\cdot K_3\right)\end{array}\right\}$	$Q_3=2\cdot K_2\cdot K_3+1.67\cdot K_1\cdot K_3+K_1\cdot K_2$
4	$\tilde{\boldsymbol{\Phi}}=\left\{\begin{array}{c}1\\ \frac{1}{Q_4}\cdot\left(\begin{array}{r}2.5\cdot K_2\cdot K_3\cdot K_4+2.25\cdot K_1\cdot K_3\cdot K_4+\\ +1.75\cdot K_1\cdot K_2\cdot K_4\end{array}\right)\\ \frac{1}{Q_4}\cdot\left(2.5\cdot K_2\cdot K_3\cdot K_4+2.25\cdot K_1\cdot K_3\cdot K_4\right)\\ \frac{1}{Q_4}\cdot\left(2.5\cdot K_2\cdot K_3\cdot K_4\right)\end{array}\right\}$	$Q_4=2.5\cdot K_2\cdot K_3\cdot K_4+2.25\cdot K_1\cdot K_3\cdot K_4$ $+1.75\cdot K_1\cdot K_2\cdot K_4+K_1\cdot K_2\cdot K_3$

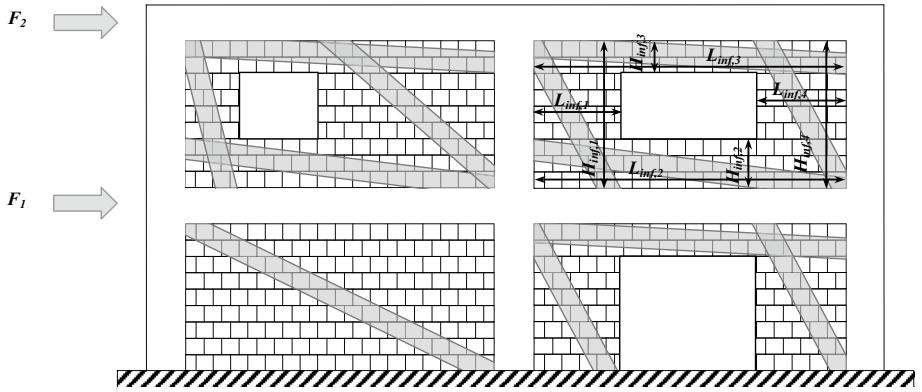

Fig. 2 Compression struts acting along masonry infills during seismic excitation (FEMA-356 2000)

Parameters in Eqs. (2) are defined as follows: A_f is the floor area, A_{col} is the column cross sectional area, $A_{inf,k}$ is the horizontal area of the k-th infill pier oriented parallel to the direction of seismic action considered, H_{cl} is the clear (deformable) height of storey columns, $H_{inf,k}$ and $L_{inf,k}$ are the height and length of the k-th infill pier (Fig. 2), E_c is the elastic modulus of concrete ($\approx 4500 \cdot \sqrt{f_c}$, where, f_c is the concrete compressive strength), h is the section height in the direction of the earthquake excitation, f_{inf} is the compressive strength of the masonry infills, $\mu_y^{\inf}$ is the level of ductility attained by the masonry infill at the point of yielding of the surrounding R.C. frame (i.e., $\mu_y^{\inf} = \theta_i / \theta_y^{\inf}$), where, $\theta_y^{\inf} \cong 0.2\%$ (Vamvatsikos and Pantazopoulou 2016), $\rho_{c,i}$ and $\rho_{inf,i}$ are the dimensionless area ratios of R.C. columns and masonry infill walls at i-th storey (i.e., $\rho_{c,i} = A_{c,i}/A_f$ and $\rho_{inf,i} = A_{inf,i}/A_f$, where, $A_{c,i}$ and $A_{inf,i}$ are the total column and masonry infill wall areas at the storey. Note that only infills oriented parallel to the seismic action are considered in this calculation). Coefficient α_c effectively reduces the elastic modulus of concrete, E_c, in order to account for the extent of cracking: $a_c = 0.33$ for very low levels of axial load ratio acting on the column, v, $(0 \le v < 0.10)$, $a_c = 0.5$ for $v \ge 0.10$, whereas, for columns in tension $a_c = 0$. Parameters D_i^c and $D_i^{\inf}$ in the stiffness term of Eq. (2a) account for contributions to stiffness both from R.C. elements and from masonry infills, according with the expression:

$$D_i^c = a_{c\_av,i} \cdot E_c \cdot \left(\frac{h_{av,i}}{H_{cl}} \right)^2; \quad D_i^{\inf} = \sum_{k=1}^{N_{\inf}} \frac{0.1 \cdot f_{\inf}}{\mu_y^{\inf} \cdot \theta_y^{\inf} \cdot \sqrt{1 + \frac{H_{\inf,k}^2}{L_{\inf,k}^2}}} = \beta \cdot \sum_{k=1}^{N_{\inf}} \frac{20 \cdot f_{\inf}}{\sqrt{1 + \frac{H_{\inf,k}^2}{L_{\inf,k}^2}}} \tag{3}$$

where, $a_{c\_av,i}$ and $h_{av,i}$ are the average values of a_c and h of the i-th storey columns and $L_{inf,i}$ is the average length of infill piers and spandrels in the i-th storey parallel to the sway direction (Fig. 2). Stiffness contribution of the infills in the floor is calculated based on the N_{inf} diagonal struts that develop from corner to corner of the piers—however if openings interrupt the continuity of a single strut, then several diagonals are included to represent the spandrels. The product $\theta_i = \mu_y^{\inf} \cdot \theta_y^{\inf}$ is the ith-storey relative drift ratio: therefore the magnitude of D_i^{inf} decays with increasing storey drift: this is reflected by the factor β, which is 1, 0.5, and 0.25 for interstorey drift ratio of 0.5%, 1% and 2%.

For buildings that do not satisfy the regularity requirement described above (e.g. buildings with torsional sensitivity, or discontinuous mass/stiffness distribution) the fundamental shape of lateral vibration may be estimated as the normalized deflected shape that the structure assumes if it is loaded laterally, in the direction of interest, by a notional gravitational field (Clough and Penzien 1975).

With the shape of lateral response already known it is easy to identify hot-spots in the building, i.e. storeys where localization of deformation demand—and therefore local failure—may be expected: these are the storeys where the difference in the shape coordinate, $\Delta\boldsymbol{\Phi}_{cr} = \boldsymbol{\Phi}_i - \boldsymbol{\Phi}_{i-1}$ within a floor, is maximum. The actual magnitudes of drift demands, may be obtained after multiplying the shape coordinates,$\tilde{\boldsymbol{\Phi}}$ with the displacement demand obtained for the estimated fundamental translational period of the building in the sway direction, T_1, from the displacement spectrum of the design hazard (for 5% damping). For example, considering Type I spectrum for Soil type B of EN 1998-1 (2004) it may be shown that the seismic demand in terms of average value of column lateral drift ratio at the building's critical storey in the examined direction is:

$$0.15\,\mathrm{s} \le T_1 \le 0.50\,\mathrm{s}: \quad \theta_{c,\mathrm{lim}} = 0.075 \cdot a_g \cdot \lambda_c \cdot \frac{\Delta\boldsymbol{\Phi}_{cr} \cdot \boldsymbol{\Phi}_s \cdot (2 \cdot \pi \cdot \Omega)^2}{H_{cl}} \cdot \frac{M_{cr}}{K_{cr}} \tag{4a}$$

$$0.50\,\mathrm{s} < T_1 \le 2.00\,\mathrm{s}: \quad \theta_{c,\mathrm{lim}} = 0.0375 \cdot a_g \cdot \lambda_c \cdot \frac{\Delta\boldsymbol{\Phi}_{cr} \cdot \boldsymbol{\Phi}_s \cdot (2 \cdot \pi \cdot \Omega)}{H_{cl}} \cdot \sqrt{\frac{M_{cr}}{K_{cr}}} \tag{4b}$$

whereas, when the displacement response spectrum of an actual earthquake excitation acting on the building is available as $S_d(T_1)$, then the drift demand is calculated as:

$$\theta_{c,\mathrm{lim}} = \lambda_c \cdot S_d\left(T_1\right) \cdot \frac{\Delta\boldsymbol{\Phi}_{cr} \cdot \boldsymbol{\Phi}_s}{H_{cl}} \tag{5}$$

In Eqs. (4) and (5), $S_d(T_1)$ is the value of the relative displacement response spectrum corresponding to the fundamental period of the building, T_1, a_g is the PGA for the site in consideration (m/s^2), M_{cr} and K_{cr} are the critical storey's mass and lateral stiffness in the sway direction (from Eq. 2a, or, 2b) and the excitation factor Φ_s, and period-parameters Ω and T_1 may be approximated from Eq. (6a) for buildings with uniform plan configuration and from Eq. (6b) for buildings with a soft-storey formation:

$$\boldsymbol{\Phi}_s = \sum_{i=1}^{N} \boldsymbol{\Phi}_i \Big/ \sum_{i=1}^{N} \boldsymbol{\Phi}_i^2; \quad \Omega = \sqrt{\sum_{i=1}^{N} \boldsymbol{\Phi}_i^2 \Big/ \sum_{i=1}^{N} \Delta\boldsymbol{\Phi}_i^2}; \quad T_1 = 2 \cdot \pi \cdot \Omega \cdot \sqrt{M_{cr} \Big/ K_{cr}} \tag{6a}$$

$$\boldsymbol{\Phi}_s = 1;\ \Omega = \sqrt{N},\ \text{where } N = \text{ number of storeys}; \quad T_1 = 2 \cdot \pi \cdot \sqrt{N} \cdot \sqrt{M_{cr} \Big/ K_{cr}} \tag{6b}$$

Ratio $\lambda_c = \lambda/(1+\lambda)$ is the moment distribution factor that accounts for the relative stiffness of the columns in a given floor as compared to the beams (in case of stiff diaphragms $\lambda_c = 1$, implying all deformation is developed in the columns; in case of stiff columns and flexible diaphragms, $\lambda_c = 0$ implying that all deformation occurs in the beams—same value holds if the beams have formed plastic hinges; an intermediate value of $\lambda_c = 0.5$ is a likely option for well designed, modern structures). Note that the value of λ_c is the average for a

given floor; its value depends on the stiffnesses of n_b beams and n_c columns converging to a frame connection (excluding cantilevering members): $\lambda = (n_b \cdot E_c \cdot I_b \cdot H_{cl}) / (n_c \cdot E_c \cdot I_c \cdot L_b)$ where $E_c \cdot I_b$ and $E_c \cdot I_c$ are the secant to yield sectional stiffnesses of these members respectively, and L_b is the typical length of beams.

2.2 Strength assessment criterion

The strength assessment criterion is a lower-bound solution motivated by concepts of capacity-based prioritizing of resistance (CBP) (Pantazopoulou and Syntzirma 2010); thus, a plausible state of equilibrium is assumed along the entire height of each column as illustrated by the assumed moment diagram under lateral sway, shown in Fig. 3. The slope of the column moment diagram within a floor is the column shear force, whereas the slope of the same diagram within the height of the beam represents the joint shear. With reference to this state of equilibrium, the column shear in any critical floor may be limited by exhaustion of any strength mechanism along the column line: several alternatives are considered in order to identify the controlling failure of the column-line (which is the lowest strength option):

F1: flexural yielding in columns;
F2: shear failure of the column web;
F3: anchorage failure of longitudinal reinforcement of the column;
F4: attainment of the development capacity of column lap splices;
F5: beam-column joint shear failure;
F6: punching failure in slab-column connections.

Also considered in establishing the hierarchy of failure is the ideal scenario of limiting the shear force input to the column, V_{by}, through ductile yielding of the longitudinal reinforcement of the adjacent beams. Clearly the implicit assumption is that a building may be deemed vulnerable (therefore warranting a second tier detailed assessment) if brittle failure dominates the response prior to the occurrence of flexural yielding even along a single column line. Comparisons are made with reference to the value of shear force magnitude in the swaying column of the critical floor in the same column line (where drift localization is evident from the shape of the fundamental swaying mode as discussed in the stiffness criterion). The column shear is calculated from the slope of the moment diagram at

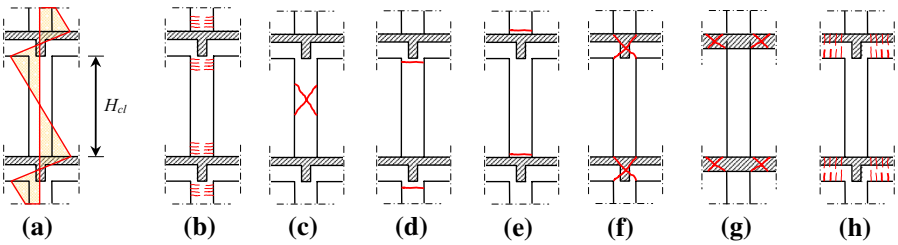

Fig. 3 **a** Static system assumed: moment distribution of an R.C. column caused by earthquake loading and **b**–**h** possible modes of failure: **b** flexural yielding; **c** shear failure; **d** anchorage failure of longitudinal reinforcement; **e** failure of lap splices; **f** beam-column joint shear failure; **g** punching failure in slab-column connections; **h** yielding of the longitudinal reinforcement of the adjacent beams (Pardalopoulos et al. 2018a)

the occurrence of each of the failure mechanisms: the source of failure is identified by the subscript in the corresponding shear value, namely, V_{flex} for F1, V_v for F2, V_a for F3, V_{lap} for F4, V_j for F5, V_{pn} for F6. These shear force values that identify the many alternative possible failure modes along a column line are calculated using the expressions provided in the "Appendix" (Pardalopoulos et al. 2013), as summarized in Table 2.

From the magnitudes of these column shear forces, corresponding resistance ratios are determined by normalizing with the column shear force associated with mechanism F1 (i.e. column flexural yielding at the critical sections, Fig. 3b) as follows: $r_v = V_v/V_{flex}$, $r_a = V_a/V_{flex}$, $r_{lap} = V_{lap}/V_{flex}$, $r_j = V_j/V_{flex}$, $r_{pn} = V_{pn}/V_{flex}$ and $r_{by} = V_{by}/V_{flex}$. The prevailing mode of failure of the examined column is identified by the resistance ratio, r_{fail}:

$$r_{fail} = min\{\, r_v,\ r_a,\ r_{lap},\ r_j,\ r_{pn} \,\} \le r_{by} \tag{7}$$

In the case where $r_{fail} = r_{by}$, plastic hinges are expected to develop in the ends of the beams adjacent to the examined column. When $r_{fail} < r_{by}$, then in the case where $r_{fail} \ge 1.0$ the column is expected to develop ductile response as the result of yielding of its longitudinal reinforcement (however, in that case, second order sway effects need be considered to anticipate possible soft-storey behaviour after flexural yielding), whereas, if $r_{fail} < 1.0$ the column is expected to fail in a brittle manner after the exhaustion of its available strength which is lower than the flexural demand.

With known limiting drift capacity of the critical columns in a structure and provided that for all column lines of this storey $r_{fail} < r_{by}$, (i.e., if failure occurs in the critical storey's columns), then Eqs. (4) and (5) may be inverted in order to calculate the limiting ground acceleration, $a_{g,lim}$ (m/s^2) that the building may tolerate without significant structural damage. If the design hazard is represented by the Type I spectrum for Soil type B of Eurocode 8-1 (EN 1998-1 2004), $a_{g,lim}$ is approximated as:

$$0.15\,\mathrm{s} \le T_1 \le 0.50\,\mathrm{s}: \quad a_{g,\mathrm{lim}} = 13.333 \cdot \left(R_{fail,cr} \cdot \frac{\theta_{c,y}}{\lambda_c} \right) \cdot \frac{H_{cl}}{\Delta\boldsymbol{\Phi}_{cr} \cdot \boldsymbol{\Phi}_s \cdot (2 \cdot \pi \cdot \Omega)^2} \cdot \frac{K_{cr}}{M_{cr}} \tag{8a}$$

$$0.50\,\mathrm{s} < T_1 \le 2.00\,\mathrm{s}: \quad a_{g,\mathrm{lim}} = 26.667 \cdot \left(R_{fail,cr} \cdot \frac{\theta_{c,y}}{\lambda_c} \right) \cdot \frac{H_{cl}}{\Delta\boldsymbol{\Phi}_{cr} \cdot \boldsymbol{\Phi}_s \cdot (2 \cdot \pi \cdot \Omega)} \cdot \sqrt{\frac{K_{cr}}{M_{cr}}} \tag{8b}$$

If, on the other hand, the spectrum of an actual seismic excitation is used to describe the hazard, then $a_{g,lim}$ can be approximated by multiplying the PGA of the earthquake record, $a_{g,o}$, with the attenuation factor $A = S_a(T_1)/S_{a,e}(T_1)$, where, $S_{a,e}(T_1)$ is the value of the elastic absolute acceleration response spectrum of the earthquake corresponding to T_1, and $S_a(T_1)$ is calculated from:

Table 2 Identifying code of plausible modes of failure along a column line

Failure mode	Flexural	Shear	Anchorage	Lap splice	Joint shear	Slab punching	Plastic hinges in beam
Notation	F1	F2	F3	F4	F5	F6	F7
Figure	3b	3c	3d	3e	3f	3g	3h
Equation	10	11	12	13	14	15	16

$$S_a(T_1) = \left(R_{fail,cr} \cdot \frac{\theta_{c,y}}{\lambda_c}\right) \cdot \frac{H_{cl}}{\Delta\Phi_{cr} \cdot \Phi_s} \cdot \left(\frac{2 \cdot \pi}{T_1}\right)^2 ; i.e., a_{g,lim} = a_{g,o} \cdot A \quad (9a)$$

In Eqs. (8) and (9), $R_{fail,cr}$ = average ($r_{fail,i}$) value of all columns in the critical storey and $\theta_{c,y}$ is the column rotation at yielding of the longitudinal reinforcement (for lack of a detailed estimate, $\theta_{c,y}$ is 0.5% for columns with usual height to sectional dimension ratio of 6, multiplied by 2/3 for stocky columns with an aspect ratio of 4 or less, and by 3/2 for slender columns with an aspect ratio of 8 or more). Note that when one or more column lines of the critical storey exhibit yielding of the longitudinal reinforcement of the adjacent beams, the product $R_{fail,cr} \cdot \theta_{c,y}/\lambda_c$ in Eqs. (8) and (9) is replaced by θ_u/λ_b where θ_u is the rotation capacity of the beam $= \mu_\theta \cdot \theta_{y,b}$ and λ_b after beam yielding may be taken ≈ 1. If beam yielding controls, the rotational ductility at the plastic hinges is estimated from the available curvature ductility using the following: $\mu_\theta = 1 + (\mu_\varphi\text{-}1) \cdot 0.5 \cdot (T_1/0.50)$ for Eq. (8a) and $\mu_\theta = 0.5 \cdot (\mu_\varphi + 1)$, for Eq. (8b), whereas $\mu_\varphi \approx b_1 \cdot 0.0035/\varepsilon_{sy}$, with b_1 ranging between 4 and 5 for usual types of beam cross sections.

An even simpler estimation may be provided in terms of available base shear coefficient that the building can support:

$$\eta = R_{fail,cr} \cdot \left[\sum_{k=1}^{N_c} V_{flex}\right] / W \quad (9b)$$

where, W is the total weight of the building (including partial contribution of live loads according with the earthquake design combination).

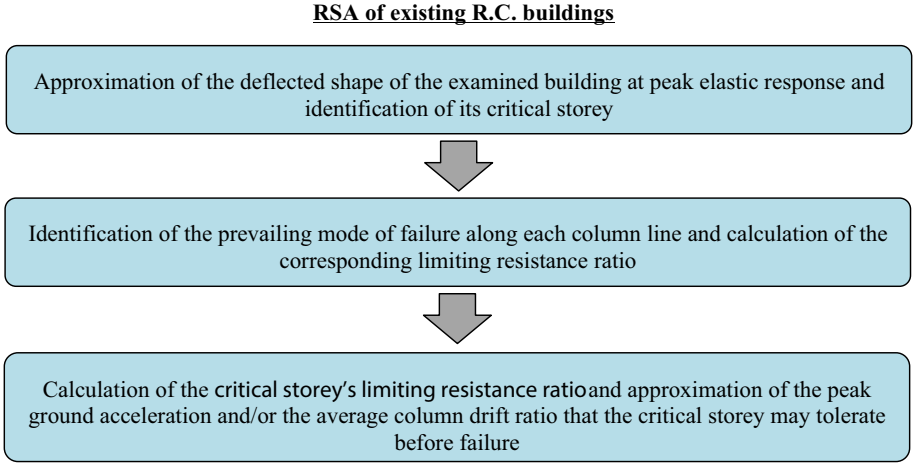

Fig. 4 Schematic representation of the RSA system

2.3 Summary of the RSA system

The two assessment criteria of the RSA system outlined in the preceding are coupled in a three-step procedure, illustrated in the flow-chart of Fig. 4.

3 Rapid seismic assessment of the icons R.C. frames

The ease of application of the method and the relevance of the calculated results is demonstrated in the present section, through its application to two full-scale, R.C. model structures, which were tested at the European Laboratory for Seismic Assessment (ELSA) in Ispra, Italy, in the framework of the ICONS TMR-Network research program (Varum 2003).

3.1 Description of the ICONS frames

The structures were practically planar reinforced concrete frames although they had a monolithically cast floor slab that cantilevered symmetrically with respect to the frame in the transverse direction. The frames modelled the design and construction practice used in R.C. buildings that were built throughout Southern Europe during the post-world II war economic development until the early 1980s. The two frames had identical R.C. structural system, comprising columns, beams and slabs (Fig. 5a). Each frame had a total length of 12.70 m and a total height of 10.80 m (storey gross height equal to 2.70 m). In all storeys a monolithically cast, 0.15 m thick slab was extending over a transverse distance of 2.00 m on each side of the frames' longitudinal axis, supported by transverse beams that converged to the frame connections. Columns C1, C3 and C4 had constant cross sectional dimensions along the height of the structure and were oriented with their strong axis perpendicular to the plane of action of the frame. Stocky column C2, the only R.C. column with the stronger axis oriented parallel to the frames' plane, had cross section dimensions of 0.60 m × 0.25 m in the first and second storeys, whereas the section height was reduced to 0.50 m in the third and fourth storey. Details regarding the cross-sectional dimensions and longitudinal reinforcement of all columns are presented in Fig. 5b. The longitudinal reinforcement of all columns had a lap splice of 0.70 m at the base of the first and the third storey, with a hook formation at the end of the bars. All columns had ∅6 mm perimeter stirrups, spaced at 0.15 m on centers. All beams parallel to the frames' plane had web cross section dimensions of 0.25 m × 0.50 m; the corresponding dimensions of the transverse beams were 0.20 m × 0.50 m. All longitudinal reinforcement and stirrups of columns and beams comprised smooth bars. Further details regarding reinforcement arrangement are available in Varum (2003). Mean concrete compressive strengths obtained from tests on cylindrical core specimens taken from the buildings after completion of the experiment, f_{cm}, was found equal to 13.90 MPa, 13.80 MPa, 9.20 MPa and 11.00 MPa for the 1st, 2nd, 3rd and 4th storey columns, respectively, whereas, from uniaxial tensile tests on steel bar coupons the yield stress of reinforcement, f_y, was found equal to 343.60 MPa.

The masonry infilled ICONS frame comprised infill walls with different types of openings, as depicted in Fig. 5a. The long external bay contained a 1.20 m × 1.00 m window opening at each of the four storeys, the central bay contained a 2.00 m × 1.75 m doorway at ground floor and a 2.00 m × 1.00 m window opening in each of the upper three

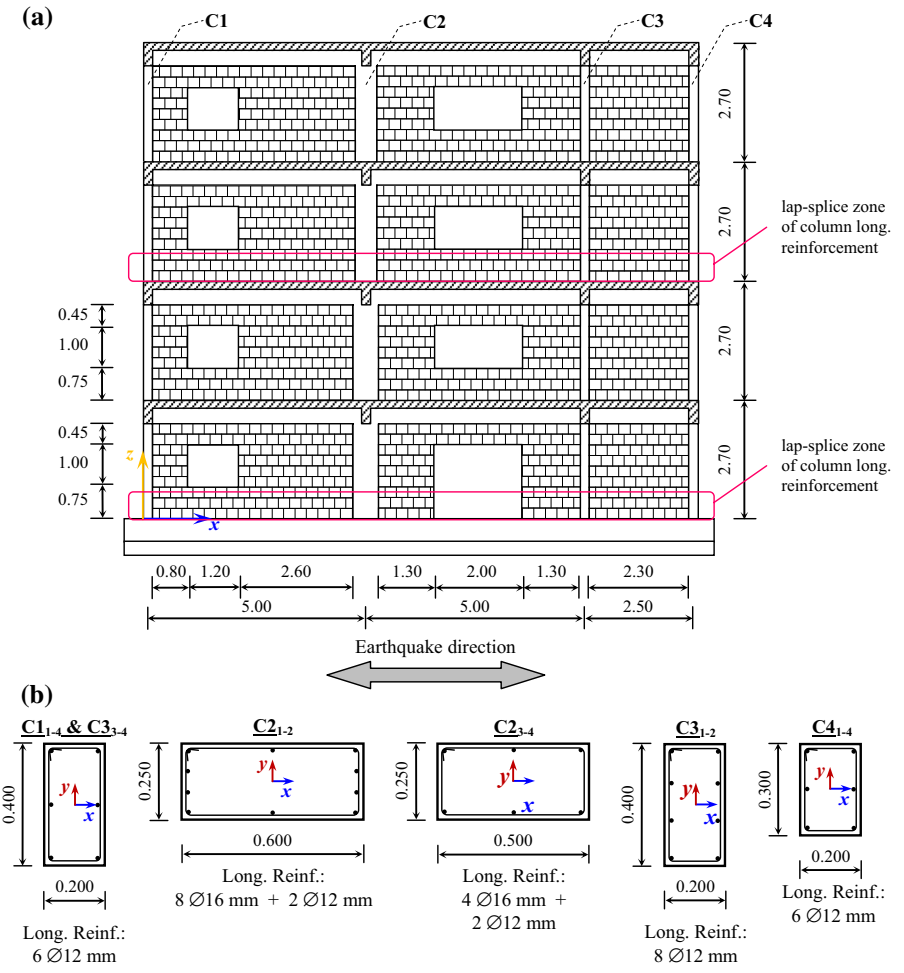

Fig. 5 The ICONS frames: **a** general layout of the frames; **b** geometric characteristics of the frames' columns (the first subscript in the columns' identification code refers to the column line, and the second subscript corresponds to the storey in which the respective cross section shown occurs)

storeys, whereas, the external short bay was fully infilled. All infill walls were single-wythe masonry with an effective thickness (i.e. the thickness of the wall excluding the thickness of plaster on each side) equal to 0.12 m.

Both ICONS frames were subjected to pseudo-dynamic testing procedures to investigate their seismic response. Each frame was successfully subjected to two artificially generated acceleration time-histories, the first with 475 year-return-period (yrp) corresponding to 2.180 m/s^2 peak ground acceleration (PGA) and the second with 975 ypr and 2.884 m/s^2 PGA (Fig. 6a), both representing a moderate-to-high European seismic hazard scenario (Varum 2003) (i.e., both records having the same waveform, frequency content and duration), whereas, the infilled frame was subjected to the first 5.00 s of a 2000 yrp acceleration time-history having a PGA of 3.728 m/s^2.

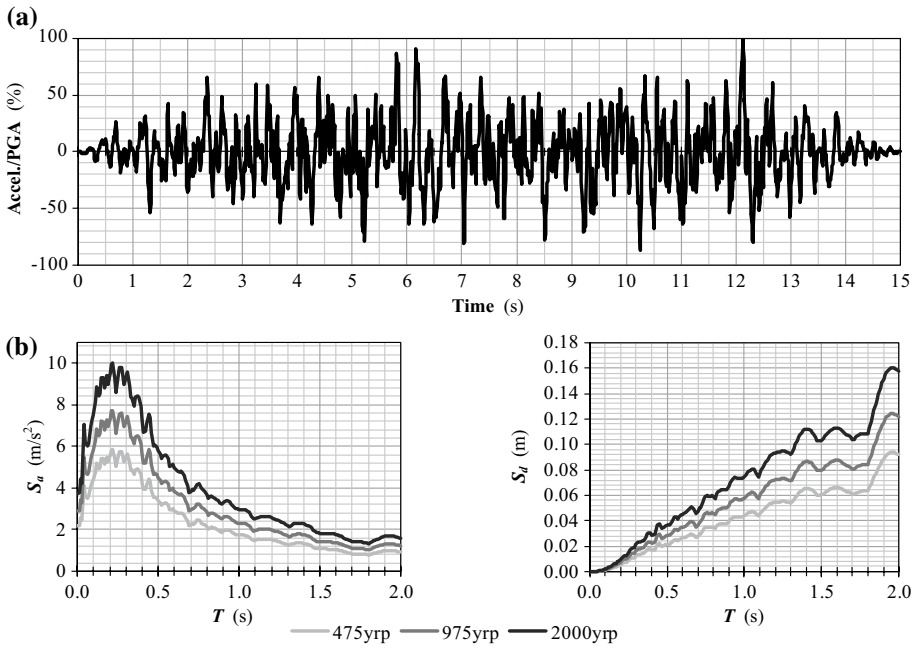

Fig. 6 Earthquake input used in the pseudo-dynamic tests of the ICONS frames: **a** acceleration time-history normalized to PGA (Varum 2003); **b** absolute acceleration, S_a, and relative displacement, S_d, response spectra for the 475 yrp, the 975 yrp and the 2000 yrp earthquake scenarios, calculated for 5% viscous damping

3.2 Stiffness assessment of the two ICONS frames

To apply the Rapid Seismic Assessment procedure, first, the normalized displacement profile (mode shape) of the ICONS frames during lateral sway is estimated so as to identify their critical storey from the tendency for localization already evident in the response shape. Given that the arrangement of the R.C. columns in the ICONS frames cannot be classified as typical, the detailed calculation of the storeys' lateral stiffness is performed according to Eq. (2b). From the values of f_{cm} listed above, the modulus of elasticity E_c ($\approx 4500 \cdot \sqrt{f_c}$ MPa) is estimated as: 16.8, 16.7, 13.6 and 14.9 GPa for the 1st, 2nd, 3rd and 4th storey columns, respectively.

With regards to the bare frame subjected to the 475 yrp and the 975 yrp earthquakes, the column axial load ratios, v, fluctuates around the mean value which corresponds to the overbearing load, as a result of the overturning action of the lateral inertia forces. To assess the dynamic behavior of the frame columns, the extreme values of axial load ratio, developing at the instant of maximum seismic response are considered (Table 3). These values were calculated from static analysis of the ICONS bare frame considering the gravity and the overturning effects of the inertial lateral loads imposed during the actual tests (Varum 2003). Considering these values of v, and consistent with the definition of column stiffness (Eq. 2b), the coefficient a_c is taken equal to 0.50 for all columns except for columns $C1_4$ and $C4_4$ in the case of the 475 yrp earthquake and for columns $C1_{1\text{-}2}$ and $C1_4$ in the case of the 975yrp earthquake, for which $a_c = 0.33$. Using these data and given the geometric properties of the structural system (i.e., for Columns $C1_{1\text{-}4}$

Table 3 Column axial load ratios, ν, of the ICONS bare frame resulting from the gravity and earthquake load combinations

Storey	Column C1		Column C2		Column C3		Column C4	
	$SW+E_{475\ yrp}$/ $SW-E_{475\ yrp}$ (kN)	$SW+E_{975\ yrp}$/ $SW-E_{975\ yrp}$ (kN)	$SW+E_{475\ yrp}$/ $SW-E_{475\ yrp}$ (kN)	$SW+E_{975\ yrp}$/ $SW-E_{975\ yrp}$ (kN)	$SW+E_{475\ yrp}$/ $SW-E_{475\ yrp}$ (kN)	$SW+E_{975\ yrp}$/ $SW-E_{975\ yrp}$ (kN)	$SW+E_{475\ yrp}$/ $SW-E_{475\ yrp}$ (kN)	$SW+E_{975\ yrp}$/ $SW-E_{975\ yrp}$ (kN)
1	0.20/0.53	0.05/0.69	0.34/0.34	0.34/0.33	0.61/0.45	0.68/0.38	0.43/0.21	0.53/0.10
2	0.17/0.37	0.08/0.46	0.26/0.25	0.26/0.25	0.44/0.34	0.48/0.30	0.30/0.17	0.37/0.11
3	0.20/0.33	0.14/0.39	0.30/0.30	0.30/0.30	0.40/0.35	0.43/0.32	0.27/0.18	0.32/0.14
4	0.08/0.11	0.07/0.12	0.12/0.12	0.12/0.12	0.15/0.13	0.15/0.13	0.09/0.07	0.10/0.07

SW are the gravity loads deriving from self weight; $E_{475\ yrp}$ $E_{975\ yrp}$ and are the axial column forces owing to the earthquake overturn, calculated from the 475 yrp and the 975 yrp earthquake cases, respectively

and $C3_{1\text{-}4}$: $A_{col}=0.080$ m^2, $h=0.20$ m; for Columns $C2_{1\text{-}2}$: $A_{col}=0.150$ m^2, $h=0.60$ m; for Columns $C2_{3\text{-}4}$: $A_{col}=0.125$ m^2, $h=0.50$ m; and for Columns $C4_{1\text{-}4}$: $A_{col}=0.060$ m^2, $h=0.20$ m; $H_{cl}=2.20$ m in all storeys), in the case of the bare frame the lateral stiffness of each storey is estimated according to Eq. 2b as: $K_{1,\mathrm{BF}}=48{,}617$ kN/m; $K_{2,\mathrm{BF}}=48{,}442$ kN/m; $K_{3,\mathrm{BF}}=25{,}669$ kN/m; $K_{4,\mathrm{BF}}=27{,}306$ kN/m. Substituting the values of $K_{1\text{-}4}$ in the appropriate expressions of Table 1 and considering that storey masses were in the case of the bare frame $M_{BF,1\text{-}3}=43.9$ ton and $M_{BF,4}=36.3$ ton, the deformed shape of the bare ICONS frame at peak seismic response for the 475yrp earthquake case is approximated as $\tilde{\boldsymbol{\Phi}}_{BF}^{T}=\{1.000, 0.819, 0.483, 0.254\}$, resulting in interstorey displacements $\Delta\tilde{\boldsymbol{\Phi}}_{BF}^{T}=\{0.181, 0.336, 0.229, 0.254\}$; this identifies the third floor as the floor where the relative normalized drift ratio is maximum (i.e. normalized relative drift ratio, $\Delta\Phi_3=0.336$, showing a tendency for localization of damage in that floor). Initially and before the estimation of the sequence of possible damage the same shape is used also to model the structural response under the 975 yrp event.

In the case of the infilled frame, the contributions of the struts developing in the masonry infills are also considered in calculating the storey lateral stiffness (see Fig. 2). Table 4 presents the geometric characteristics of the segments of the masonry infills defined around the openings as illustrated in Fig. 2 and according to FEMA 356 (2000). The fully developed model is shown in Fig. 7; the struts effectively increase the storey lateral stiffness as compared to the bare frame. The compressive strength of the masonry infills, as determined from tests conducted on separate infill samples (Varum 2003), was $f_{mw}=1.1$ MPa. Assuming $\mu_{y,mw}\cdot\theta_{y,mw}=0.5\%$ in all storeys (i.e. assuming that the concrete frame elements yield at an average storey drift of about 0.5% and that the masonry infills have attained a ductility of about 2.5 at the onset of yielding of the encasing frame), the lateral stiffness of the frame's storeys explicitly owing to masonry infills is approximated

Table 4 Geometric characteristics of the struts modelling masonry infill action as per Fig. 7

Storey	Infill section	L_{inf} (m)	$A_{inf}=(L_{inf}\cdot t_{inf})$ (m^2)	H_{inf} (m)
1	1-Left	0.80	0.10	2.20
	1-Right	2.60	0.31	2.20
	1-Top	4.60	0.55	0.45
	1-Bottom	4.60	0.55	0.75
	2-Left	1.30	0.16	2.20
	2-Right	1.30	0.16	2.20
	2-Top	4.60	0.55	0.45
	3	2.30	0.28	2.20
2–4	1-Left	0.80	0.10	2.20
	1-Right	2.60	0.31	2.20
	1-Top	4.60	0.55	0.45
	1-Bottom	4.60	0.55	0.75
	2-Left	1.30	0.16	2.20
	2-Right	1.30	0.16	2.20
	2-Top	4.60	0.55	0.45
	2- Bottom	4.60	0.55	0.75
	3	2.30	0.28	2.20

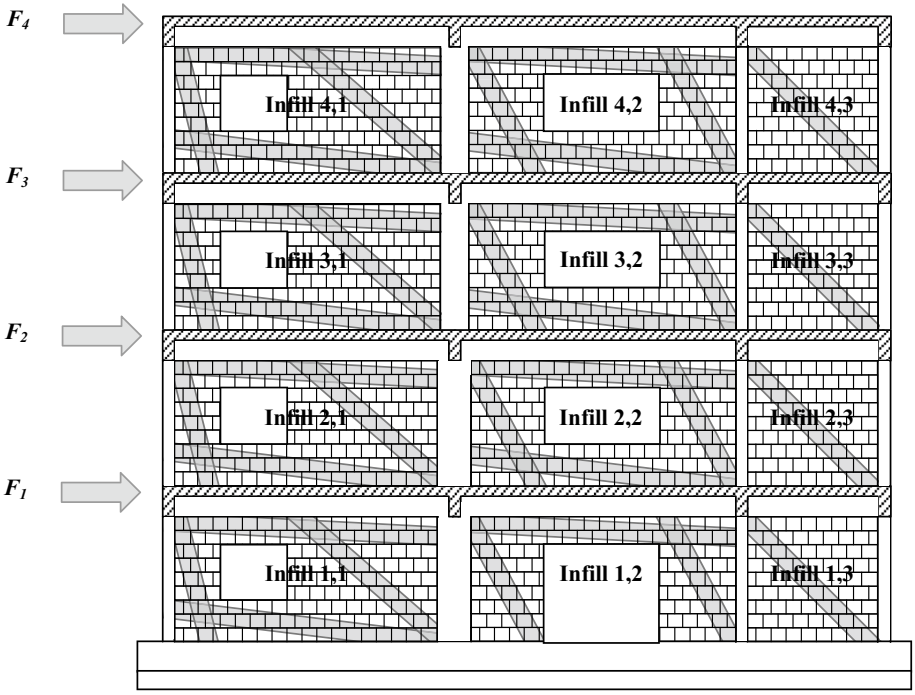

Fig. 7 Formation of compression struts acting along the infills of the ICONS frame when subjected to earthquake loading as per the FEMA 356 (2000) guideline

from the last term of Eq. (2b) as $K_1^{\inf}=22{,}727$ kN/m and $K_{2,4}^{\inf}=28{,}175$ kN/m. Considering that the axial load ratio of the infilled frame columns was similar to that of the bare frame columns (Table 3) and that the total lateral stiffness of each storey of the infilled ICONS frame equals to the sum of the lateral stiffness owing to its R.C. columns and to that owing to its masonry infills, it follows that: $K_{1,\mathrm{IF}}=71{,}345$ kN/m, $K_{2,\mathrm{IF}}=76{,}617$ kN/m, $K_{3,\mathrm{IF}}=53{,}844$ kN/m and $K_{4,\mathrm{IF}}=55{,}481$ kN/m. Given that the storey masses of the infilled frame were $M_{\mathrm{IF},1\text{-}3}=45.5$ ton and $M_{\mathrm{IF},4}=37.5$ ton respectively, according to Table 1 it is shown that: $\tilde{\boldsymbol{\Phi}}_{IF}^{T}=\{1.000, 0.843, 0.560, 0.305\}$ and $\Delta\tilde{\boldsymbol{\Phi}}_{IF}^{T}=\{0.157, 0.283, 0.255, 0.305\}$, identifying the first floor as the critical storey (normalized relative drift ratio $\Delta\Phi_1=0.305$, showing the greatest tendency for localization.) At higher levels of lateral drift the ductility attained by the infills may be well beyond the value of 2.5 mentioned above and therefore their strength can no longer be sustained. At that stage, the contribution of the infills can be assumed as diminished particularly in the most affected floors (i.e. floors where the normalized relative drift ratio is maximum—here in the first floor), with the response inevitably tending towards a shear building profile.

Figure 8 presents a comparison between the estimated (from the RSA procedure) deformed shape of both ICONS frames and their recorded peak seismic storey-drift profile during the 475yrp event (Varum 2003)—note that in the later case the values of inter-storey drift correspond to the performance limit state at the onset of localization of failure in the critical R.C. members which is the performance state considered in the RSA procedure.

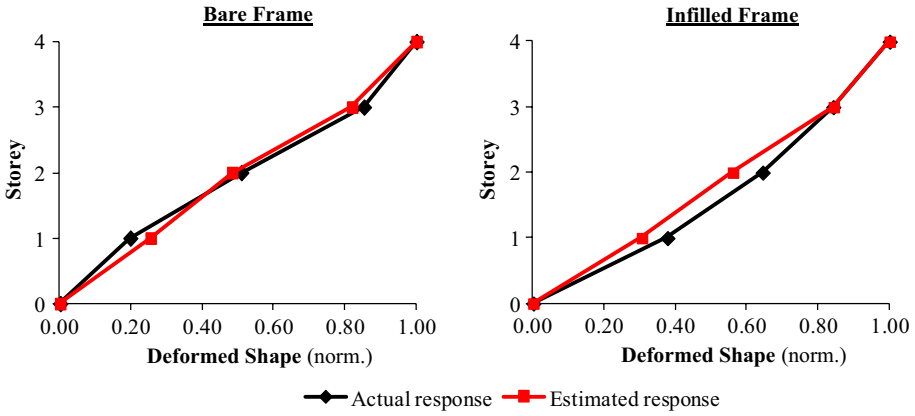

Fig. 8 Comparison between the deformed shape of the ICONS buildings at peak lateral response, estimated according to the RSA procedure (red line) and the actual experimental response from the first, 475yrp event (black line)

As illustrated in Fig. 8, in both building cases the estimated deformed shape is in very good agreement with the actual seismic response both with regards to the locations of the developed damages (i.e. the third storey in the case of the bare and the first storey in the case of the infilled frame) and the relative intensity of localization.

3.3 Strength assessment of the ICONS frames

The second step in applying the RSA procedure in the case of the two ICONS frames is strength assessment along the R.C. column lines. Since the geometric and material characteristics of the R.C. structural system of both bare and infilled frames were identical, the results of the strength assessment apply to both cases.

Application of the strength assessment procedure requires the determination of the shear strength of all column lines corresponding to all plausible failure mechanisms (Table 2) and their structural system configuration. An application example of the strength assessment procedure for column C1 of the first storey ($C_{1,1}$) is as follows: Section height in the direction of earthquake excitation was 0.200 m, the column effective depth was $d=0.158$ m, $b=0.400$ m, and the column had deformable length $H_{cl}=H_{storey}-h_{beam}=2.70-0.50=2.20$ m. Furthermore, $A_{s,tot}=6\cdot(\pi\cdot0.012^2/4)=6.79\times10^{-4}$ m^2, leading to $\rho_{\ell,tot}=0.0107$. Considering the $SW+E_{475yrp}$ earthquake combination, the column axial load ratio equals to $v_{C1\text{-}1}=0.20$ (Table 2), corresponding to a normalized depth of compression zone $\xi=0.432$ (based on sectional analysis as per Chapter 4 of FIB Bulletin 24, 2003). Substituting to Eq. (10) of the "Appendix" ($f_c^{'}=13.90$ MPa; $f_y=343.60$ MPa) the shear strength that column $C_{1,1}$ could develop if yielding of its longitudinal reinforcement was the prevailing mechanism of failure would be $V_{flex\text{-}C1,1}=25.44$ kN. The shear strength of column $C_{1,1}$ due to exhaustion of its web shear strength, $V_{v\text{-}C1,1}$, is determined from Eq. (11b), since $v_{C1\text{-}1}>0.10$. To do so, the angle of sliding plane, θ_v, is calculated from linear interpolation as: $\theta_{v\text{-}C1,1}=35°$. Considering that $\tan\alpha_{C1,1}=0.066$, leading to $a_{C1,1}=4°$ ($<\theta_{v\text{-}C1,1}$) and that $A_{tr}=2\cdot(\pi\cdot0.006^2/4)=0.57\times10^{-4}$ m^2 (perimeter stirrups), $f_{st}=343.60$ MPa and $s=0.150$ m, $V_{v\text{-}C1,1}=35.72$ kN. Lap failure of longitudinal reinforcement of column $C_{1,1}$ is determined from Eq. (13), considering $\mu_{fr}=0.3$, $L_{lap}=0.700$ m; $a_b=0$ (smooth reinforcement bars);

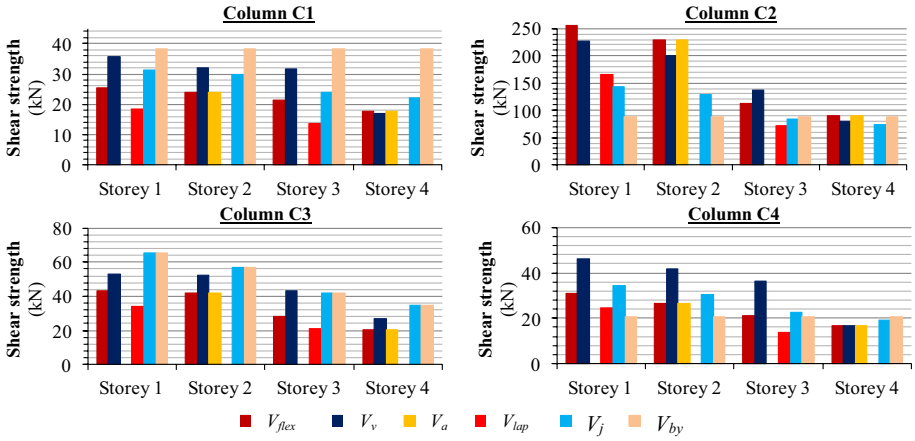

Fig. 9 Shear forces at failure modes of all storey columns of both ICONS frames calculated for the case of the $SW + E_{475yrp}$ event

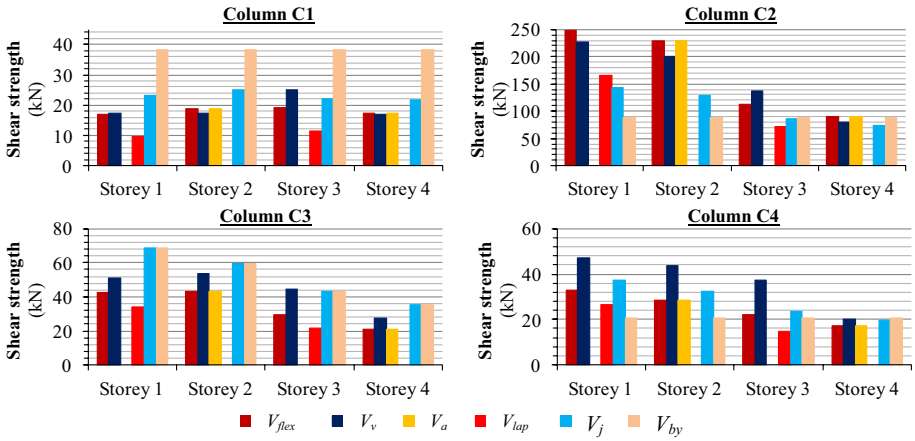

Fig. 10 Shear forces at the failure modes of all storey columns of both ICONS frames calculated at their terminal performance level

$N_b = 3$; $A_b = 1.13 \times 10^{-4}$ m^2; $D_b = 0.012$ m; $f_t = 0.3 \times 13.90^{2/3} = 1.73$ MPa; $a_{hook} = 1$; $f_b = 2 \cdot [0.90 \cdot (13.90/20)^{0.5}] = 1.80$ MPa, as $V_{lap\text{-}C1,1} = 18.45$ MPa. Beam-column joint shear failure of column $C_{1,1}$ is calculated for $\gamma_j = 1.0$, $v_{j\text{-}C1,1} = 0.20$ (Table 2), $d_{beam} = 0.458$ m and $b_j = 0.325$ m, according to Eq. (14a), as: $V_{j\text{-}C1,1} = 31.43$ kN. Finally, given that $\rho_{beam} = 0.0055$, the limiting shear input to column $C_{1,1}$ due to yielding of longitudinal reinforcement of the adjacent beams parallel to the frame direction equals to $V_{by\text{-}C1,1} = 38.20$ kN. Figures 9 and 10 present the values of shear forces thus estimated for the various modes of failure of each column line and for the $SW + E_{475yrp}$ event and at the terminal performance level of both frames (the $SW + E_{975yrp}$ event in the case of the bare and the $SW + E_{2000yrp\text{-}first\_5s}$ event in the case of the infilled frame) –these load combinations were needed in order to calculate the axial loads bearing on the columns-, whereas Figs. 11 and 12 illustrate the corresponding resistance ratios. Similar results derive from

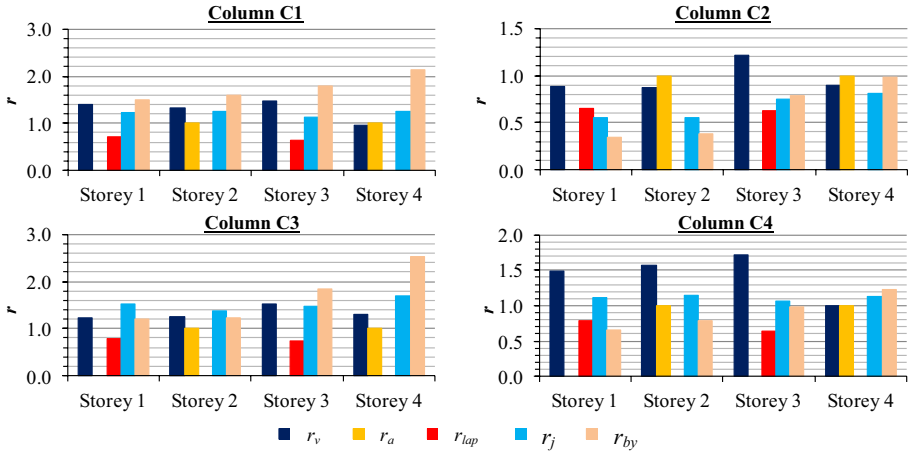

Fig. 11 Resistance ratios of all storey columns of both ICONS frames calculated for the case of the SW + E_{475yrp} event

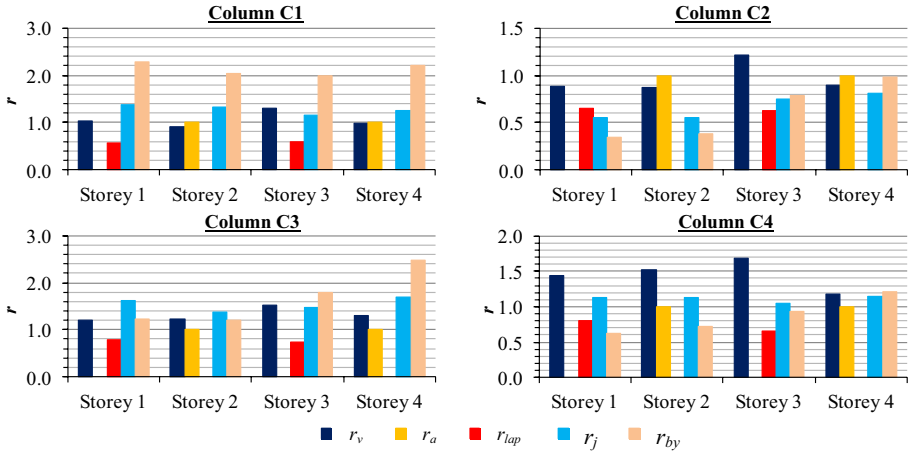

Fig. 12 Resistance ratios of all storey columns of both ICONS frames at their terminal performance level

application of the RSA strength assessment in the cases of the SW-E_{475yrp}, SW-E_{975yrp} and SW-$E_{2000yrp\text{-}first\_5s}$ earthquake cases.

According to the RSA results, the magnitudes of the shear force capacities of the various modes of failure of the ICONS frames differ between the 475yrp event and their terminal performance level (also resulting in different magnitudes of resistance rations, *r*) due to the different levels of the fluctuating column axial loads. Yet, the hierarchy between all possible failure modes that may develop at the individual columns of the ICONS frames remains the same in both earthquake scenarios considered. To this end, for the first storey, failure in columns $C_{1,1}$ and $C_{3,1}$ is controlled by the lap splice development capacity of primary reinforcement at the base of the columns, whereas, the shear force in columns $C_{2,1}$ and $C_{4,1}$ is limited by plastic hinge formation in the adjacent beams. In the case of the second storey column $C_{1,2}$ is at the margin between flexural yielding and shear failure of its web, column

$C_{3,2}$ is controlled by flexural yielding and columns $C_{2,2}$ and $C_{4,2}$ are expected to behave similarly as in the first storey. With regards to the third storey, all columns are expected to develop failure of their primary reinforcement lap splices, whereas, in the fourth storey all columns are expected to behave similarly as in the second storey, except of the column $C_{2,3}$ which is controlled by its joint shear strength. Lap-splice failure was actually reported for the third-storey columns of the bare frame (Varum 2003).

3.4 Estimation of the ICONS frames' seismic response at the onset of failure in the critical R.C. members

The final step in applying the RSA procedure is the approximation of the limiting lateral drift ratio and peak ground acceleration that the critical storey of the ICONS frames may tolerate before failure.

First the 475 yrp event is considered consistent with the sequence of occurrence during the tests. The period of the fundamental translational mode of vibration of the two ICONS frames in their plane of action, T_1, is approximated first. Parameter Φ_s is 1.298 and 1.281 in the cases of the bare and the infilled frame, respectively, whereas, $\Omega_{BF}=2.738$ and $\Omega_{IF}=2.831$. Considering that the masses of the frames' critical storey were, $M_{BF,3}=43.9$ ton and $M_{IF,1}=45.5$ ton, according to Eq. (6a), it is estimated that $T_{1,BF}=0.71$ s and $T_{1,IF}=0.45$ s, in the cases of the bare and the infilled frames, respectively. For these values of T_1, in the case of the 475yrp earthquake the spectral absolute acceleration for the bare and the infilled frames is equal to $S_{a,e}(T_1)_{475\text{-BF}}=2.292$ m/s^2 and $S_{a,e}(T_1)_{475\text{-IF}}=4.315$ m/s^2 and the relative displacements at the top floor equal to $S_d(T_1)_{475\text{-BF}}=29$ mm and $S_d(T_1)_{475\text{-IF}}=22$ mm (Fig. 6b).

The seismic demand of the two frames is determined in terms of average value of column drift of the frames' critical storey (3rd and 1st for the BF and IF, respectively). Considering the geometry of the columns and beams, the typical connection distribution factors for C1, C2, C3 and C4 columns are: For the first and the second storey $\{\lambda_{c,C1}=0.86;\ \lambda_{c,C2}=0.43;\ \lambda_{c,C3}=0.94;\ \lambda_{c,C4}=0.94\}$, for the third storey $\{\lambda_{c,C1}=0.86;\ \lambda_{c,C2}=0.56;\ \lambda_{c,C3}=0.94;\ \lambda_{c,C4}=0.94\}$ and for the fourth storey $\{\lambda_{c,C1}=0.93;\ \lambda_{c,C2}=0.72;\ \lambda_{c,C3}=0.97;\ \lambda_{c,C4}=0.97\}$. Thus, for the critical storey of the bare frame (the third storey), the fraction of the total storey drift that corresponds to the storey's columns is the average value $\lambda_{c\text{-BF,cr}}=(0.86+0.56+0.94+0.94)/4=0.83$, whereas, at the first storey of the infilled frame beam yielding occurs. Therefore, while the masonry walls still contribute to the first storey stiffness, it may be assumed that the distribution factor $\lambda_{c\text{-IF,cr}}$ tends to 0 for the upper-end of the first-storey columns, whereas the formation of beam plastic-hinge mechanism depends on the formation of hinges at the lower end of the columns, at the base. (Furthermore, if the masonry wall contribution is diminished due to damage the first storey becomes a soft-storey mechanism and therefore, at that stage, it would be $\lambda_{c\text{-IF,cr}}\approx 1$; this means that the structural model used to derive the shape of lateral response may have to be modified in order to account for this sequence of failure).

3.4.1 Seismic response of the bare frame

Considering the assumed deformed shape of the ICONS frames at peak seismic response, in the case of the 475yrp earthquake scenario the seismic demand in terms of average column drift ratio in the critical storey (the third floor) of the bare frame can be approximated

according to Eq. (5) as: $\theta_{c,lim}=(\lambda_{c\text{-BF,cr}}=0.83)\cdot(S_d(T_1)_{475\text{-BF}}=0.029)\cdot(\Delta\Phi_3=0.336)\cdot(\Phi_s=1.298)/(H_{cl}=2.20)=0.48\%$.

The drift capacity of the columns of the ICONS bare frame's critical storey (i.e., 3rd floor) before lap-splice failure equals to $R_{fail,cr}\cdot\theta_y$, where, $R_{fail,cr}$ is the average of the r_{fail} values of all columns in the critical storey and θ_y may be approximated in the case of the slender R.C. columns as $(3/2)\cdot0.5\%=0.75\%$. According to Figs. 11 and 12, in the case of the bare frame the product $R_{fail,cr\text{-BF}}\cdot\theta_{y,c}$ is estimated from: $R_{fail,cr\text{-BF}}=\text{ave}\{0.60, 0.63, 0.74, 0.66\}=0.66$, leading to seismic drift capacity of its critical storey (3rd storey) equal to $0.66\cdot0.75\%=0.50\%$, This corresponds to 104% of the seismic demand of the 475yrp earthquake—thus, according to the RSA, lap splice failure is imminent at the 3rd floor of the bare frame, although the sustained damage is limited. This result is consistent with the experimental reports from inspection of the bare frame after the 475 ypr event (Varum 2003).

The intensity of earthquake ground acceleration associated with the onset of localization of failure in the R.C. members in the critical (third) floor, $a_{g,lim}$, is approximated using Eq. (9). As previously calculated, for the critical storey of the bare frame (the 3rd storey) the storey resistance ratio is $R_{fail,cr\text{-BF}}=0.66$, which according to Eq. (9a) leads to $S_a(T_1)_{\text{BF}}=2.34$ m/s^2. By scaling the earthquake spectra used for the excitations (Fig. 6b) to the calculated values for $T_{1\text{-BF}}=0.71$ s ($A_{\text{BF-475yrp}}=2.34/2.29=1.02$) it is found that the maximum tolerable ground acceleration for the bare ICONS frame is $a_{g,lim\text{-BF,475yrp}}=2.18\cdot1.02=2.22$ m/s^2, practically coinciding with the value associated with $T_1=0.71$ s of the 475yrp event used in the tests.

3.4.2 Seismic response of the infilled frame

In the case of the infilled frame, the critical storey (1st storey) is expected to sustain the seismic demand since at its critical storey yielding of longitudinal reinforcement of the beams converging in the joint connection of the stocky column C2 prevails practically precluding the development of all brittle mechanisms of column failure. Therefore, in the case of the 475yrp earthquake scenario the seismic demand in terms of average storey drift ratio in the critical storey (the first floor) of the infilled frame can be approximated according to Eq. (5) as:

$$\theta_{c,lim}=(S_d(T_1)_{475-IF}=0.022)\times(\Delta\Phi_3=0.305)\times(\Phi_s=1.281)/(H_{cl}=2.20)=0.39\%,$$

which is again below the damage limit of either beams or the base of columns in first floor. At that stage the masonry infills have attained a ductility of almost 2; and apart from cracking in the infills, no significant damage would be anticipated in the overall frame, consistently with the experimental observations.

3.5 Estimation of the ICONS frames' seismic response at their terminal performance level

As previously identified from the procedure of stiffness assessment, the critical storey of the ICONS specimens is the 3rd storey in the case of the bare frame and the 1st storey in the case of the infilled frame. Furthermore, performance of the proposed strength assessment procedure highlighted that the prevailing failure mode of the R.C. structural system of the bare frame is failure of lap splice of the longitudinal reinforcement in all columns of the 3rd storey, whereas in the case of the infilled frame, yielding of longitudinal reinforcement

of the 1st storey beams converging in the joint connection of the stocky column C2 prevails, practically precluding the development of all brittle mechanisms of column failure at the top of the columns so long as the masonry infills sustain their contribution whereas due to the stiffness provided by the infills, the rotation demand at the column bottom were still below the failure limit of 0.5% (estimated earlier to correspond to lap splice failure).

For the terminal performance level of the ICONS bare frame to be assessed by the RSA method, the compliance created in the 3rd floor due to lap splice cracking should be accounted for in the structural model before assessing the response for the subsequent 975 yrp event. (Note that the PGA of the 975 yrp event was 33% higher than that of the 475 yrp event; as failure in the lap splices was imminent in the end of the 475-yrp event, it was the first likely mode of failure for the stronger event). To reproduce this modification of response, rotational hinges are introduced at the base of the third storey columns in the analytical model of the structure; in that case, the storey stiffness of the third floor is reduced to a quarter of the original value, to $K_{3,\mathrm{BF}} = 25{,}669/4 = 6417$ kN/m (on account of the hinges forming at the lap splices of the third storey columns reducing the stiffness from $12EI_y/H^3$ to $3EI_y/H^3$). Calculation of Φ according to Table 1 changes into: $\tilde{\Phi}^T_{BF} = \{1.000, 0.910, 0.240, 0.126\}$, which illustrates how drift demand in that floor is exacerbated further in the subsequent seismic event leading to further localization of deformation demand and damage, with the corresponding normalized relative displacement demand, $\Delta\Phi_3$ (i.e. the shape coordinate difference for the 3rd floor) being increased to $0.67 = 0.91 - 0.24$. For the revised shape function of lateral response, the corresponding value of Φ_s is 1.197, whereas $\Omega_{\mathrm{BF}} = 1.979$ and the period of the damaged frame is estimated as, $T_{1,\mathrm{BF}} = 1.03$ s.

Terminal testing of the infilled frame was conducted using a 2000 yrp event, with a PGA value scaled to 3.728 m s^{-2}. If it is assumed that due to limited damage reported in the 475-yrp event no significant change had occurred in the dynamic characteristics of the infilled frame, then it would follow that the corresponding relative spectral displacement for this acceleration level would be, $S_d(T_1 = 0.45\ \mathrm{s})_{2000\text{-IF}} = 0.038$ m as illustrated in the displacement spectra of Fig. 6b. Therefore the corresponding drift ratio in the first floor would equal to 0.67%, which corresponds to severe damage of the masonry infills and lap splice cracking at the base of the columns. At that advanced drift level it is clear

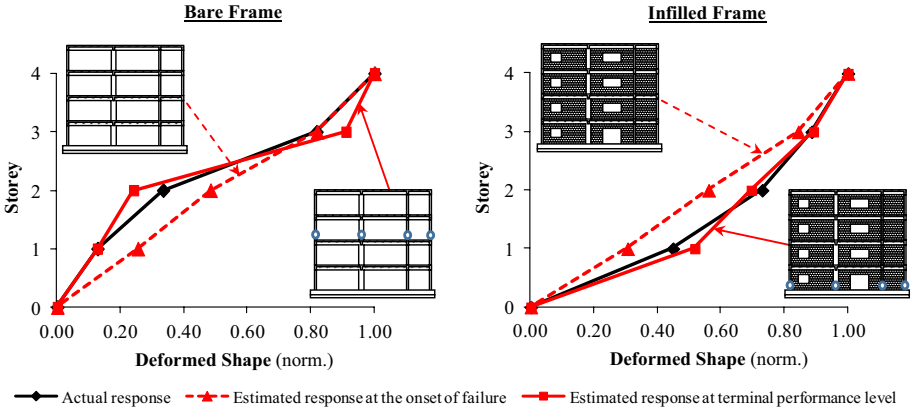

Fig. 13 Comparison between the estimated deflected shapes of the two ICONS frames at the onset of structural damage and at terminal performance level with their actual peak seismic response

that the first storey struts may be reduced through the β factor in Eq. (3): ($\beta = 0.75$ by interpolation); whereas hinges are introduced at the base of the first story column to account for the splice failure (i.e., column stiffness is reduced to ¼ of the original value). This leads to ($K_1^{\inf} = 0.75 \times 22{,}727 = 17{,}000$ kN/m), and $K_{1,\text{IF}} = (48{,}617/4) + 17{,}000 = 29{,}150$ kN/m. Therefore, the revised deflected shape Φ is $\tilde{\Phi}_{IF}^{T} = \{1.000, 0.891, 0.695, 0.517\}$, indicating a tendency for soft-storey formation in the first floor ($\Delta\Phi_1 = 0.517$) and an increased period of $T_1 = 0.66$ s; parameter $\Omega_{\text{IF}} = 2.69$, and $\Phi_s = 1.219$.

Figure 13 illustrates the difference between the first round estimate of Φ and its approximation at terminal response of both ICONS frame, as well as the comparison of these shapes with the actual peak response of both ICONS frames recorded during the strongest earthquake test of the test campaign (the 975 yrp earthquake in the case of the bare and the 2000yrp earthquake in the case of the infilled frame).

In light of the findings of the revised models of the two frames after consideration of terminal damage, a final step in applying the RSA procedure is to approximate the limiting lateral drift ratio that the critical storey of the ICONS frames could tolerate before failure. With the increased period values displacement demand is also increased and localization in the critical floors is exacerbated further owing to the commensurate increase of the respective $\Delta\Phi$ value. Thus, for the 975 yrp earthquake it is, $S_{a,e}(T_1 = 1.03\text{ s})_{975\text{-BF}} = 2.4$ m/s^2; $S_d(T_1 = 1.03\text{ s})_{975\text{-BF}} = 60$ mm, and $S_{a,e}(T_1 = 0.66\text{ s})_{2000\text{-IF}} = 4.8$ m/s^2, and $S_d(T_1 = 0.66\text{ s})_{2000\text{-IF}} = 52$ mm (Fig. 6b). Again, the intensity of seismic demand of the two frames is quantified in terms of average value of column drift of the frames' critical storey (3rd and 1st for the BF and IF, respectively).

Considering that columns are the vulnerable element in the critical storey of the bare frame (i.e., 3rd storey), the fraction of the total storey drift that corresponds to the storey's columns is taken the same as in the 475 yrp event: $\lambda_{c\text{-BF,cr}} = 0.83$. The seismic demand in terms of average column drift ratio in the critical storey of the bare frame is approximated according to Eq. (5) as: $\theta_{c,lim} = 0.83 \times 0.06 \times (0.67 \times 1.197)/2.20 = 1.8\%$. This is excessive rotation at the plastic hinges that occurred at the base of the third storey columns, responsible for the excessive damage observed during the tests at that location (rotation ductility of 3.5). Similarly in the infilled frame, the hinges at the base of the first storey columns experience a rotation demand of: $\theta_{c,lim} = 1.0 \cdot 0.052 \cdot (0.517 \cdot 1.219)/2.20 = 1.4\%$; this drift level corresponds to excessive infill damage that cannot be sustained by the single-wythe infills (an infill ductility demand of 7), and a ductility of about 2.8 at the base of the first storey columns.

3.6 Discussion of assessment results

According to the damage inspections conducted at the end of the pseudo-dynamic tests using the 475yrp earthquake record (PGA = 2.180 m/s^2) the bare frame exhibited slight cracks, not clearly visible, that did not require any type of repair, whereas, the infilled frame exhibited minor damages only at the infills, including minor cracking around openings and separation between the infill panels and the surrounding frames (Varum 2003). Yet, after the end of the pseudo-dynamic tests using in the case of the bare frame the 975 yrp earthquake record (PGA = 2.884 m/s^2) and in the case of the infilled frame the 2000 yrp earthquake record (PGA = 3.728 m/s^2) both frames exhibited heavy damages, which are illustrated in Fig. 14.

The comparison between the damage patterns observed after the two pseudo-dynamic tests and the results of the RSA prove the dependability of the procedure. In both cases

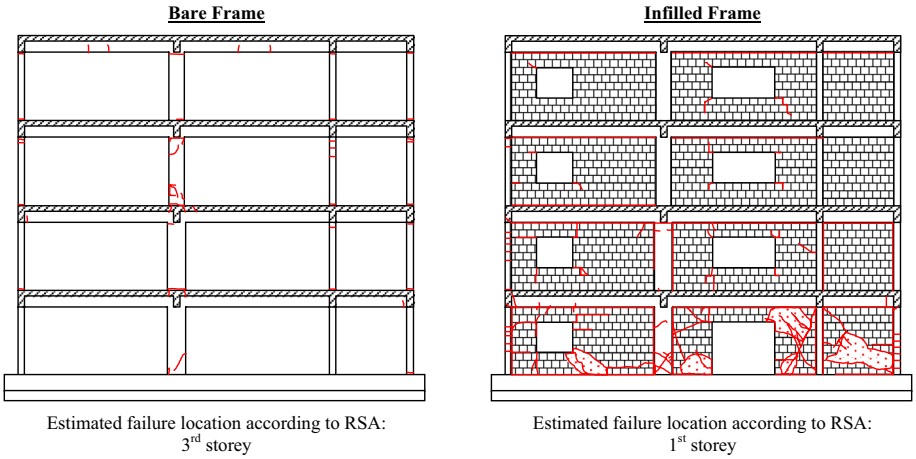

Fig. 14 Damage patterns observed at the bare frame after the 975 yrp earthquake of 2.884 m/s^2 PGA and at the infilled frame after the first 5 s of the 2000 yrp earthquake of 3.728 m/s^2 PGA and comparison with the results estimated according to the RSA procedure

considered, the RSA successfully identified the critical storey of the frame as well as the damage patterns along the columns and the beams of the entire structural system, whereas, it approximated with exceptional accuracy the peak ground acceleration that the frame could sustain without developing any damages (RSA approximated $a_{g,lim}=2.22$ m/s^2 whereas the actual damages of the bare frame developed at a PGA little over 2.18 m/s^2). The procedure's accuracy is also evident by comparing its results with the observed responses of the two frames at the subsequent stronger event, both in terms of identifying the frame's critical storey as well as the drift demand and ensuing damage.

4 Conclusions

Practical implementation of a Rapid Seismic Assessment procedure (RSA) that could be used in pre-earthquake screening of existing R.C. buildings is illustrated. The method combines a lower bound equilibrium criterion for identifying the weakest failure mechanism that controls the lateral response of the structure, with a stiffness criterion that identifies the anticipated seismic demand from the design hazard spectra. The method is further improved by the introduction of closed form expressions for approximating the deflected shape of the examined buildings at peak seismic response, which is essential for localization of demands and for identification of the critical floors in the building. To this end, the accuracy and objectivity of RSA estimates is improved without compromising the versatility of the approach.

To illustrate the practical implementation of the RSA procedure, the method is used in the paper for damage assessment of case studies concerning two full scale, planar R.C. buildings that have been tested at the ELSA Laboratory under simulated strong ground motions with PGA of 0.22 g and 0.29 g. This application, which also serves as a practical guide for interested users, highlights the accuracy of the RSA procedure through comparisons of the estimated results (both in terms of drift demands, prevailing mode of failure and anticipated damage) with the actual seismic response of the examined buildings.

The buildings chosen for the study presented interesting features: one (a bare frame) was controlled by failure in a higher floor where a point of stiffness discontinuity localized the demands, whereas the other (a frame with masonry-infilled floors) was controlled by localization of the lowest storey. The method proved successful both in estimating the anticipated response of the buildings' structural elements near failure under lateral sway, as well as in identifying the tendency for damage localization (i.e. the critical storey) of each structure and in approximating the limiting lateral column drift and the limiting ground accelerating that the building could tolerate before failure.

Furthermore, the RSA method successfully assessed the seismic response of both frames at terminal performance level, after having been subjected to sequential earthquakes that caused damages and effectively altered their structural system.

Results obtained from the rapid methodology correlate very well with those obtained from the tests while requiring minimal, transparent calculations. Nevertheless, the method is approximate in nature and as such, blind correlations with field observations and tests are needed to further illustrate any possible limitations that may arise from the simplifying assumptions and approximations made in its application.

Appendix

The individual strength terms of an R.C. column can be calculated using the following expressions, which represent the present state of the art at the field. Nevertheless, these expressions may be subject to change as the knowledge base in reinforced concrete leads to improved models for the individual mechanisms of resistance.

Flexural shear demand

$$V_{flex} = \left[\rho_{\ell,tot} \cdot \frac{f_y}{f_c} \cdot (1 - 0.4 \cdot \xi) + v \cdot \left(\frac{h}{d} - 0.8 \cdot \xi\right)\right] \cdot \frac{b \cdot d^2 \cdot f_c}{H_{cl}} \tag{10}$$

Exhaustion of shear strength

$$\text{If } v < 0.10: \quad V_v = A_{tr} \cdot f_{st} \cdot \frac{d \cdot (1 - 0.4 \cdot \xi)}{s} \cdot \cot\theta_v \tag{11a}$$

$$\text{If } v \geq 0.10: \quad V_v = v \cdot b \cdot d \cdot f_c \cdot \tan\alpha + A_{tr} \cdot f_{st} \cdot \frac{d \cdot (1 - 0.4 \cdot \xi)}{s} \cdot \cot\theta_v \tag{11b}$$

Anchorage failure of longitudinal reinforcement

$$V_a = \left[\rho_{\ell,tot} \cdot \frac{\min\left\{\frac{4 \cdot L_a \cdot f_b}{D_b} + \alpha_{hook} \cdot 50 \cdot f_b \;;\; f_y\right\}}{f_c} \cdot (1 - 0.4 \cdot \xi) + v \cdot \left(\frac{h}{d} - 0.8 \cdot \xi\right)\right] \cdot \frac{b \cdot d^2 \cdot f_c}{H_{cl}} \tag{12}$$

Lap failure of longitudinal reinforcement

$$V_{lap}=\frac{\left[\min\left\{\left(\mu_{fr}\cdot L_{lap}\cdot\left[\frac{A_{tr}}{s}\cdot f_{st}+\alpha_b\cdot\left(b-N_b\cdot D_b\right)\cdot f_t\right]+\right.\right.\right.\left.\left.\left.+\alpha_{hook}\cdot 50\cdot N_b\cdot A_b\cdot f_b\right)\;;\;N_b\cdot A_b\cdot f_y\right\}\cdot d\cdot(1-0.4\cdot\xi)+\right.\left.+\nu\cdot b\cdot d^2\cdot f_c\cdot(0.5\cdot h/d-0.4\cdot\xi)\right]}{H_{cl}/2} \tag{13}$$

Shear capacity of joints

$$\text{Unreinforced or lightly reinforced joints}: \quad V_j=\gamma_j\cdot 0.5\cdot\sqrt{f_c}\cdot\sqrt{1+\frac{v_j\cdot f_c}{0.5\cdot\sqrt{f_c}}}\cdot\frac{b_j\cdot d\cdot d_{beam}}{H_{cl}} \tag{14a}$$

$$\text{Well reinforced joints}: \quad V_j=\left[\gamma_j\cdot 0.5\cdot\sqrt{f_c}\cdot\sqrt{1+\frac{v_j\cdot f_c}{0.5\cdot\sqrt{f_c}}}\cdot\frac{b_j\cdot d\cdot d_{beam}}{H_{cl}}\right]\cdot\sqrt{1+\rho_{j,horiz}\cdot\frac{f_{st}}{f_t}} \tag{14b}$$

Punching shear of slab-column connections

$$V_{pn}=\frac{0.12\cdot\min\left\{1+\sqrt{\frac{200}{d_{sl}}}\;;\;2\right\}\cdot\left(100\cdot\rho_{\ell,sl}\cdot f_c\right)^{1/3}\cdot d_{sl}\cdot 0.25\cdot u_{crit}\cdot\left(h+4\cdot d_{sl}\right)}{H_{cl}} \tag{15}$$

Limiting shear due to yield of beams' longitudinal reinforcement

$$V_{by}=\frac{0.85\cdot\rho_{beam}\cdot b_{beam}\cdot d_{beam}^2\cdot f_y^{beam}}{H_{cl}} \tag{16}$$

where,

- $\rho_{\ell,tot}=A_{s,tot}/(b\cdot d)$ is the total longitudinal reinforcement ratio of a column with external dimensions $h\times b$,
- $A_{s,tot}$ is the total area of the longitudinal reinforcement at the column's critical section,
- d is the column effective depth,
- f_y is the longitudinal reinforcement yield stress,
- f_c is the concrete compressive strength,
- ξ $(=x/d)$ is the normalized depth of compression zone,
- ν is the axial load ratio acting on the cross section $(N_{g+0.3q}/(b\cdot d\cdot f_c))$,
- H_{cl} is the column's deformable length,
- $\tan\alpha=(h/d-0.8\cdot\xi)\cdot d/H_{cl}$, where a $(\leq\theta_v)$ is the angle of inclination of the diagonal strut created between the centroids of the compression zones at the top and bottom column cross sections of the column (this represents the strut forming by the axial load acting on the column according to (Priestley et al. 1996),
- θ_v $(=\{45^\circ$ when $\nu<0.10$, 30° when $\nu\geq 0.25$, whereas for $0.10\leq\nu<0.25$ θ_v is calculated from linear interpolation$\}$) is the angle of sliding plane (i.e. θ_v is the angle forming between the longitudinal member axis and a major inclined crack developing in the

plastic hinge region of the column). It determines the number of stirrup legs that are intersected by the inclined sliding plane,

- h_{st} is the height of the stirrup legs,
- A_{tr} is the total area of stirrup legs in a single stirrup pattern, which are intersected by the inclined sliding plane,
- s is the stirrup spacing,
- f_{st} is the stirrup yield stress,
- L_{α} is the anchorage length of the longitudinal reinforcement,
- D_b is the diameter of longitudinal reinforcing bars,
- α_{hook} is a binary index (1 or 0) to account for hooked anchorages ($\alpha_{hook}=0 \Longrightarrow$ no hooks),
- $f_b=2\cdot f_{b,o}$ is the concrete bond stress, where $f_{b,o}=n_1\cdot(f_c/20)^{0.5}$, $n_1=\{1.80$ for ribbed bars; 0.90 for smooth bars$\}$.
- μ_{fr} is the friction coefficient ($0.2\leq\mu_{fr}\leq 0.3$ for smooth bars; $1.0\leq\mu_{fr}\leq 1.5$ for ribbed bars),
- L_{lap} is the lap-splice length,
- α_b is a binary index (1 or 0) depending on whether ribbed or smooth reinforcement has been used,
- N_b is the number of longitudinal bars in tension,
- A_b is the area of a single tension bar,
- $f_t=0.3\cdot f_c^{2/3}$is the concrete tensile strength,
- $\gamma_j=\{1.40$ for interior joints; 1.00 for all other cases, whereas, for joints without stirrups these values are reduced to 0.4 and 0.3 respectively$\}$,
- v_j is the (service) axial load acting on the bottom of the column adjusted at the top of the joint (compression positive),
- $b_j=(b+b_{beam})/2$ is the joint width, where b_{beam} is the web width of the adjacent beam,
- d_{beam} is the beam depth,
- $\rho_{j,horiz}=A_{tr}/(s\cdot b_j)$,
- d_{sl} is the slab depth,
- $\rho_{\ell,sl}$ is the total slab reinforcement ratio at the critical punching perimeter around the column, u_{crit}
- ρ_{beam} is the tension longitudinal reinforcement ratio of the beam (i.e. the total longitudinal reinforcement ratio of the beam section adjacent to the column if an interior connection is considered, or in the case of exterior connections the value of the top or bottom beam reinforcement ratio (whichever is largest)),
- f_y^{beam} is the yield stress of the beam longitudinal reinforcement.

References

Clough RW, Penzien J (1975) Dynamics of structures, 1st edn. McGraw-Hill Inc., New York

EN 1998-1 (2004) Eurocode 8—Design of structures for earthquake resistance—part 1: general rules, seismic actions and rules for buildings. European Committee for Standardization (CEN), Brussels

EN 1998-3 (2005) Eurocode 8—design of structures for earthquake resistance—part 3: assessment and retrofitting of buildings. European Committee for Standardization (CEN), Brussels

FEMA P-154 (2015) Rapid visual screening of buildings for potential seismic hazards: a handbook. Federal Emergency Management Agency (FEMA), Washington, DC

FEMA-356, Prestandard (2000) Commentary for the seismic rehabilitation of buildings. Federal Emergency Management Agency (FEMA), Washington, DC

FIB Bulletin 24 (2003) Seismic assessment and retrofit of reinforced concrete buildings, State-of-art report prepared by Task Group 7.1. Federation of Structural Concrete (FIB)
Greek Code of Structural Interventions 2012 (2012) Earthquake planning and protection organization of Greece (E.P.P.O.), Athens
Gülkan P, Sozen MA (1999) Procedure for determining seismic vulnerability of building structures. ACI Struct J 96(3):336–342
Gür T, Pay AC, Ramirez JA, Sozen MA, Johnson AM, Irfanoglu A, Bobet A (2009) Performance of school buildings in Turkey during the 1999 Düzce and the 2003 Bingöl earthquakes. Earthq Spectra 25(2):239–256. https://doi.org/10.1193/1.3089367
Initial Evaluation Procedure (IEP) Assessment (2017). New Zealand Society for Earthquake Engineering (NZSEE), Structural Engineering Society (SESOC) and NZ Geotechnical Society (NZGS). http://www.EQ-Assess.org.nz
Japan Building Disaster Prevention Association (JBDPA) (2001) Standard for seismic evaluation and guidelines for seismic retrofit of existing reinforced concrete buildings (English Edition)
Kappos AJ, Panagopoulos G, Panagiotopoulos C, Penelis G (2006) A hybrid method for the vulnerability assessment of R/C and URM buildings. Bull Earthq Eng 4(4):391–413. https://doi.org/10.1007/s10518-006-9023-0
Pantazopoulou SJ, Syntzirma DV (2010) Deformation capacity of lightly reinforced concrete members–comparative evaluation. In: Fardis M (ed) Advances in performance-based earthquake engineering. Geotechnical, geological and earthquake engineering, vol 13. Springer, Dordrecht, pp 359–371. https://doi.org/10.1007/978-90-481-8746-1_34
Pardalopoulos S, Thermou GE, Pantazopoulou SJ (2013) Screening criteria to identify brittle R.C. structural failures in earthquakes. Bull Earthq Eng 11:607–636. https://doi.org/10.1007/s10518-012-9390-7
Pardalopoulos SI, Pantazopoulou SJ, Lekidis VA (2018a) Simplified method for rapid seismic assessment of older R.C. buildings. Eng Struct 154:10–22. https://doi.org/10.1016/j.engstruct.2017.10.052
Pardalopoulos SI, Pantazopoulou SJ, Thermou GE (2018b) Seismic rehabilitation of substandard R.C. buildings with masonry infills. J Earthq Eng. https://doi.org/10.1080/13632469.2018.1453397
Priestley MN, Seible F, Calvi GM (1996) Seismic design and retrofit of bridges. Wiley, New York
Shiga T, Shibata A, Takahashi T (1968) Earthquake damage and wall index of reinforced concrete buildings. In: Proceedings of the Tohuku district symposium, archit. Institute of Japan, vol 12, pp 29–32
Thermou GE, Pantazopoulou SJ (2011) Assessment indices for the seismic vulnerability of existing R.C. buildings with masonry infill walls. Earthq Eng Struct Dyn 40(3):293–313. https://doi.org/10.1002/eqe.1028
Vamvatsikos D, Cornell CA (2002) Incremental dynamic analysis. Earthq Eng Struct Dyn 31(3):491–514. https://doi.org/10.1002/eqe.141
Vamvatsikos D, Pantazopoulou SJ (2016) Simplified mechanical model to estimate the seismic vulnerability of heritage unreinforced masonry buildings. J Earthq Eng 20(2):298–325. https://doi.org/10.1080/13632469.2015.1060583
Varum H (2003) Seismic assessment, strengthening and repair of existing buildings. Dissertation, Universidade de Aveiro
Yakut A (2004) Preliminary seismic performance assessment procedure for existing RC buildings. Eng Struct 26(10):1447–1461. https://doi.org/10.1016/j.engstruct.2004.05.011
Yakut A, Gülkan P, Sadik Bakir B, Tolga Yilmaz M (2005) Re-examination of damage distribution in Adapazari: structural considerations. Eng Struct 27(7):990–1001. https://doi.org/10.1016/j.engstruct.2005.02.001